Emerging Contaminants 11 (2025) 100551

Contents lists available at ScienceDirect

Emerging Contaminants

journal homepage: www.keaipublishing.com/en/journals/emerging-contaminants

In-vitro metabolites characterization of 1,3-diphenylguanidine and 1,3-di-o-tolylguanidine by high-resolution mass spectrometry and urinary profiling

Andrea Estévez-Danta *, Iago Riveiro, María Lage-Díaz, José Benito Quintana, Rosa Montes, Rosario Rodil **

Aquatic One Health Research Center (ARCUS) & Department of Analytical Chemistry, Nutrition and Food Chemistry, R. Constantino Candeira S/N, IIAA building, Universidade de Santiago de Compostela, 15782, Santiago de Compostela, Spain

ARTICLE INFO

Article history:
Received 28 March 2025
Received in revised form
13 August 2025
Accepted 14 August 2025
Available online 23 August 2025

Keywords:
Rubber leachates
In-vitro metabolism
Human liver microsomes
Suspect screening
In-vivo metabolites

ABSTRACT

The discovery of the hazardous effects associated with the polymer additives 1,3-diphenyl guanidine (DPG) and 1,3-di-o-tolylguanidine (DTG) has prompted the need for biomonitoring studies to detect human exposure. However, limited information is available about their metabolism. To address this gap, this study investigates the Phase I and II *in-vitro* biotransformation of both chemicals using human liver microsomes and cytosol. The samples were analyzed using liquid chromatography coupled to high resolution-(tandem) mass spectrometry through suspect (of *in-silico* predicted metabolites) and non-target screening. The analysis revealed four Phase I and two Phase II metabolic products for both DPG and DTG. Hydroxylation of the benzene ring led to the tentative identification of mono- and di-hydroxylated metabolites. Subsequent Phase I deamination followed by oxidation resulted in the formation of hydroxy-phenylurea and an intramolecular cyclization resulted in the formation of hydroxy-cyclic products. Furthermore, N-glucuronidation and O-glucuronidation products were identified for the first time. After performing urinalysis, DPG and DTG could be quantified in the 0.02–0.23 μg L^{-1} range, and DPG-227 (mono-hydroxylated DPG) was estimated to be present at ca. 0.01–0.10 μg L^{-1} range, using DPG response as quantification surrogate. Finally, toxicity assessment using an *in-silico* tool indicated the need to consider these human metabolites in (eco)toxicological assessments, as they may have the same or even greater effects on humans and the environment.

1. Introduction

1,3-Diphenyl guanidine (DPG) and 1,3-di-o-tolylguanidine (DTG) are rubber additives widely used during the vulcanization process. Consequently, they are commonly present in products such as tires, footwear, gloves and high-density polyethylene materials. Only in the European Economic Area, the annual production and/or importation is estimated to range from 10,000 to 100,000 tons for DPG and 10–100 tons for DTG [1,2]. These compounds are known for their properties as persistent and mobile (PMT) or very persistent and very mobile (vPvM) chemicals, which contribute to their presence in the aquatic environment [3,4]. During the product life cycle, these substances can be easily released into the surrounding environment. In addition, their use in household, packaging, or consumer products (e.g. tires and recycled rubbers) leads to migration into the indoor environment, where they are detected at high levels in dust [5] and across various environmental matrices [6–8]. However, there is very limited information available on the potential impact on human health.

From a toxicological perspective, DPG and DTG are known to cause allergic contact dermatitis, especially after occupational exposure [9]. Moreover, DPG is suspected to be an endocrine disrupting chemical, although the latest evaluation report conducted by European Chemicals Agency (ECHA) in 2020 did not yield definitive conclusions regarding its reproductive toxicity [10,11]. Nevertheless, there have been few studies developed to assess

* Corresponding author.
** Corresponding author.
E-mail addresses: andreaestevez.danta@usc.es (A. Estévez-Danta), rosario.rodil@usc.es (R. Rodil).

Peer review under the responsibility of KeAi Communications Co., Ltd.

https://doi.org/10.1016/j.emcon.2025.100551

human exposure. Furthermore, human biomonitoring studies on these substances have used, so far, DPG and DTG themselves as biomarkers in urine [12], which may overlook exposure and is more problematic in terms of background contamination since these diarylguanidines might come from different sources and contaminate the biological samples.

In-vitro human liver metabolism is a methodology that has been used for decades to simulate the complex metabolic transformations that occur in human metabolism in an inexpensive, rapid and non-invasive manner, as an alternative to *in-vivo* studies. With this purpose, specific subcellular liver fractions, namely human liver microsomes (HLM) and cytosol fractions (HLCYT), along with cofactors (e.g. 2,5-uridinediphosphate glucuronic acid, UDPGA) and the target compound are mixed in a buffer solution and incubated during several hours at 37 °C [13,14]. Only two studies in literature have assessed the metabolism of diarylguanidines. One study was an *in-vitro* study with rats and rabbit liver microsomes for a group of N,N-diphenylguanidines, and the other was an *in-vivo* study with rats for DPG [15,16]. The *in-vitro* study reproduced only Phase I metabolism processes, proposing O-hydroxylation in the benzene ring for non-fluorinated guanidines and N-hydroxylation for fluorinated guanidines as potential metabolic reactions using nuclear magnetic resonance and a Vacuum Generators 7070H mass spectrometer [15]. The *in-vivo* study demonstrated that DPG was easily absorbed and distributed in various tissues in rats. Three metabolites were excreted in urine, but no structures were proposed due to insufficient data for accurate structural determination [16]. Thus, there is still a lack of evidence on which metabolites derive from both compounds.

Thus, this study carrying out Phase I and Phase II *in-vitro* assays for DPG and DTG using human liver microsomes (HLM) and cytosol fractions (HLCYT), is the first one that provides solid structural information of six biotransformation products of each of the compounds using high-resolution mass spectrometry (HRMS). The samples were then analyzed using ultra-high performance liquid chromatography-quadrupole-time of flight-(tandem) mass spectrometry (U(H)PLC-QTOF-MS/MS). Both suspect and non-target screening workflows were employed to identify and characterize potential metabolites. Finally, human pooled urine samples were used to validate the *in-vitro* findings. Furthermore, an *in-silico* toolbox was used to predict chemical (eco)-toxicity.

2. Materials and methods

2.1. Chemicals and reagents

Analytical standards of DPG and DTG were supplied by Sigma-Aldrich (Burlington, MA, USA). The analytical reference standard of irbesartan-d4 (Ib-d4) used as internal standard (IS) was purchased from Toronto Research Chemicals (North York, ON, Canada). Pooled HLMs (mixed gender, n = 50, 20 mg mL^{-1}) and pooled HLCYT (mixed gender, n = 200, 10 mg mL^{-1}) were obtained from Tebubio (Barcelona, Spain). UDPGA (98–100 %), adenosine-3′-phosphate 5′-phosphosulfate lithium salt hydrate (PAPS, >60 %), alamethicin (>98 %), phenacetin (>98 %), 4-nitrophenol (4-NP, >99 %), magnesium chloride (>98 %), sodium chloride (99.5 %) and Trizma base (>99.9 %) were supplied by Sigma-Aldrich. NADPH tetrasodium salt hydrate (>96 %) was purchased from Roche Diagnostics GmbH (Mannheim, Germany). LC-MS grade methanol (MeOH), LC-MS grade acetonitrile (ACN), dimethyl sulfoxide (DMSO), LC-MS grade formic acid, LC-MS grade acetic acid, ammonia in MeOH (7 N), NH_3 solution in water (25 %) and hydrochloric acid (37 %) were purchased from Sigma-Aldrich. Ultrapure water was obtained with a Genie Water System from RephiLe Bioscience (Boston, MA, USA).

A 100 mM TRIS buffer was prepared by dissolving 1.22 g of Trizma base and 0.11 g of $MgCl_2$ in 100 mL of ultrapure water. Then, pH was adjusted to 7.5 at 37 °C by adding 1 M HCl solution [17].

2.2. In-vitro human liver metabolism study

Fig. 1 depicts the schematic workflow for conducting experimental *in-vitro* metabolism assays, a methodology optimized and employed in previous studies with few changes [17–19]. In brief, the *in-vitro* Phase I metabolism involved two sets of samples (Sets A and B) exclusively performing Phase I reactions and other two sets (Sets C.1 and C.2) for Phase I + II reactions, each comprising three replicates. The reaction mixture was prepared by combining 945 μL of TRIS buffer (100 mM), 25 μL of HLM (20 mg mL^{-1}) and 10 μL of either DPG or DTG stock solution (1000 ng μL^{-1} prepared in DMSO) in 1.5 mL Eppendorf tubes. Set A, (Phase I-1h) was incubated for 1 h, while Sets B (Phase I-3h) and C.1 and C.2 (Phase I + II) were incubated for 3 h at 37 °C. Two incubation times (1 and 3h) have been used in the Phase I reactions to potentially identify reaction intermediates that allow us to understand the metabolic pathways of the target diarylguanidines. During the incubation time, 10 μL of NADPH (0.1 M stock solution in TRIS buffer) were added as a cofactor at 5, 60 and 120 min of incubation. The cofactor needs to be re-incorporated every hour of incubation due to its loss of activity by precipitation. Finally, the reaction in Sets A and B was stopped by adding 250 μL of a mixture of 1 % formic acid and Ib-d4 (5 ng μL^{-1}) in ACN after 1 or 3 h of incubation, respectively. Ib-d4 was chosen as IS because it was a solution available at that time in the laboratory that can be measured with good sensitivity in both electrospray positive and negative ionization modes. Samples from Set C.1 and C.2 were placed on ice for 30 s, followed by centrifugation at 8000 rpm for 5 min. Subsequently, 935 μL of the resulting supernatant were transferred to an empty Eppendorf tube.

At the same time, two new sets of samples (Sets D.1 and D.2), were prepared to carry out exclusively Phase II metabolism (n = 3). These new sets consisted of 935 μL of TRIS buffer and 10 μL of either DPG or DTG stock solution (1000 ng μL^{-1} prepared in DMSO). Sets C.1 and D.1 underwent Phase II conjugation through glucuronidation (GLU) and Sets C.2 and D.2 through sulfation (SUL) (Fig. 1). For GLU in both Sets (C.1 and D.1), 25 μL of HLMs (20 mg mL^{-1}) and 10 μL of alamethicin (1 mg mL^{-1} prepared in DMSO) were added to the samples prior to their incubation at 37 °C. During incubation, the coenzyme UDPGA (10 μL of 100 mM stock solution in TRIS buffer) was added in intervals of 5, 60, and 120 min. For SUL in both Sets (C.2 and D.2), 25 μL of HLCYT (20 mg mL^{-1}) were added to the samples before incubation. After 5, 60, and 120 min of incubation, coenzyme PAPS (10 μL of 10 mM stock solution in TRIS buffer) was introduced. After 3 h of incubation, both sets were terminated by adding 250 μL of a mixture containing 1 % formic acid and Ib-d4 (5 ng μL^{-1}) in ACN.

Prior to their injection into the LC-HRMS system, all samples were centrifuged at 8000 rpm for 5 min. The supernatant was then transferred to vials and filtered through 0.22 μm PVDF syringe-driven filters (Merck Millipore, MA, USA).

2.3. In-vivo validation through urine analysis

Urine samples were obtained through a collaboration with the General Directorate for Public Health of the Galicia regional Government – *Xunta de Galicia* (Norwest Spain) as detailed in Ref. [20]. Briefly, 435 urine samples were anonymously collected from regional government public servants in Santiago de Compostela (Spain) together with a short survey. The study was approved by the Research Ethics Committee of the Xunta de Galicia (Code 2019/

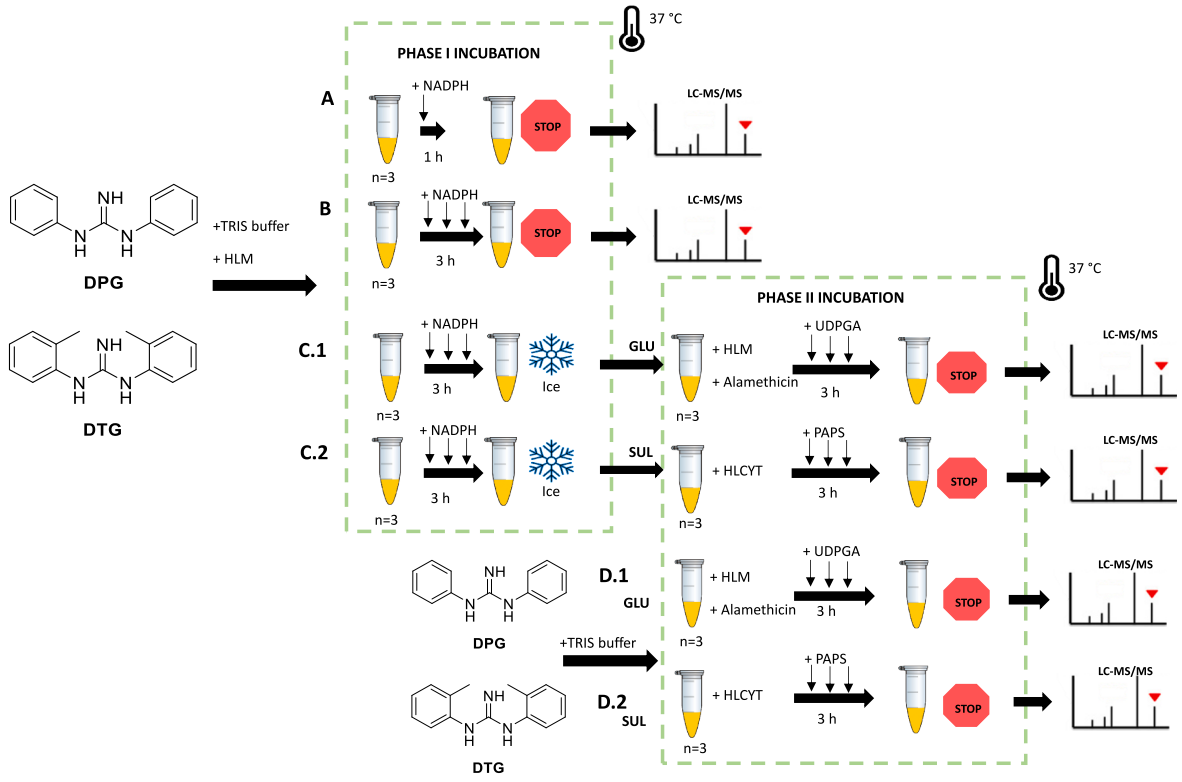

Fig. 1. *In-vitro* human liver metabolism assay overview.

545) and it had been conducted in conformity with the declaration of Helsinki. All participants provided informed written consent before their participation in the study.

Four pools of 20 urine samples were used for this study divided by sex and residential environment. Pool 1 from male and rural population, pool 2 from male and urban population, pool 3 from female and rural population, and pool 4 from female and urban population. These four urine pools were also incubated with β-glucuronidase to deconjugate Phase II metabolites, according the protocol presented in Ref. [20], and labelled as pools 1d, 2d, 3d and 4d. Non-deconjugated pools were diluted (1:4 with ultrapure water) to be comparable to the deconjugated sets in terms of dilution.

DPG and DTG concentrations in pooled urine samples were calculated by the standard addition method. Briefly, each pool of urine samples was spiked with a standard mix of both diarylguanidines in the range 0.005–0.400 μg L^{-1} (5 levels) and injected in an LC-triple quadrupole (QqQ) MS/MS system together with the corresponding non-spiked level of each pooled sample.

2.4. Instrumental analysis

Extracts collected from the *in-vitro* metabolism assay were analyzed with an Agilent 1290 Infinity II LC (Agilent Technologies, Santa Clara, CA, USA) equipped with a binary solvent pump, a thermostatted LC column compartment, and a sample manager. The U(H)PLC system was interfaced to an Agilent 6550 iFunnel QTOF system furnished with a Dual Agilent Jet Stream electrospray (ESI) ion source. Chromatographic separation was achieved on a ZORBAX Extend-C18 column (50 × 2.1 mm I.D., 1.8 μm particle size) from Agilent Technologies, with a dual eluent system consisting of (A) 5 mM ammonium acetate in ultrapure water and (B) 5 mM ammonium acetate in MeOH at a flow rate of 0.4 mL min^{-1}. The gradient was as follows: 0 min (2 % B), 1 min (2 % B), 15 min (70 % B), 16 min (70 % B), 19 min (100 % B), 20 min (100 % B), 20.01 min (2 % B) and 25 min (2 % B). The injection volume was set at 2 μL.

The QTOF-HRMS system was operated in either positive or negative mode (separate injections) in the 2 GHz (extended dynamic range) mode, providing a Full Width at Half Maximum (FWHM) resolution of ca. 12,000 at *m/z* 121 and ca. 23,000 at *m/z* 922. Capillary, nozzle and fragmentor voltage were set at 2500, 0 and 120 V, respectively. The ions 121.0508 and 922.0097 for positive mode and 112.9856 and 980.0164 for negative mode were selected for a continuous recalibration during the run to ensure mass accuracy. Nitrogen was used as nebulizing (30 psi), drying (12 L min^{-1} and 200 °C), sheath gas (9 L min^{-1} and 300 °C) and collision gas. Acquisition parameters were set for the range *m/z* from 20 to 1000 at a scan rate of 6.00 spectra s^{-1} for MS and MS/MS spectra using a data-dependent acquisition method (Auto MS/MS) with an isolation width of 1.3 amu and three collision energies (10, 20 and 40 V), with a maximum of three precursor ions per cycle. Additionally, Target MS/MS was also employed for selected ions to obtain the MS/MS spectra (conditions analogous to Auto MS/MS) in separate injections when needed. Data were stored in centroid mode. Instrument control was performed using Agilent MassHunter Workstation software B.10.00 (Agilent Technologies).

Urine samples were initially analyzed with the above LC-HRMS instrument and later with an Agilent Infinity 1290 II HPLC coupled to an Agilent 6495 triple quadrupole (QqQ) equipped with an ESI source, ought to its much better sensitivity. The analytical method and further details employed with this system can be found in Text S1 and Table S1.

2.5. Data analysis

This study was carried out employing both suspect and non-target screening approaches.

2.5.1. Suspect screening of predicted metabolites

Data processing and analysis for the suspect screening workflow was conducted with MassHunter Profinder 8.0 and MassHunter Qualitative Analysis 10.0 software, both developed by Agilent Technologies.

Initially, a list of potential metabolites was generated for both DPG and DTG by conducting a literature review on *in-vitro* metabolism or degradation of the target compounds [15,16,21], using three open-access *in-silico* prediction software tools, QSAR Toolbox, Biotransformer and GloryX [22–24], and self-proposal considering typical metabolic reactions and the structures of the precursor compounds. This suspect list contained the molecular formulae, exact mass and the source from which the metabolite was proposed. Each suspect metabolite was identified by a potential name using the precursor name abbreviation followed by their corresponding nominal mass. This information was stored in a csv-database (Tables S2 and S3).

Chromatograms were processed with the MassHunter Profinder software by applying the algorithm *Batch Targeted Feature Extraction* which extracts the *m/z* of the suspect list of the allowed adducts of the compounds ($[M+H]^+$, $[M+Na]^+$, $[M+K]^+$ and $[M + NH_4]^+$ in positive ionization, or $[M - H]^-$ in negative ionization) and further aligns the chromatographic peaks and MS/MS spectra of each sample. Subsequently, MS/MS spectra for the detected metabolites were extracted using the *Find by Auto MS/MS* or *Find by Target MS/MS* algorithms in MassHunter Qualitative Analysis Workstation.

The identification of potential *in-vitro* metabolites in both software relied on the accurate mass of precursors in MS mode, along with their corresponding fragmentation pathways. The selection criteria in MS mode included: (1) ensure a maximum mass error of ±5 ppm; (2) verify the absence of identified metabolites in the negative controls or their presence with a peak area less than 10 % of the peak area in the sample; (3) confirm the presence of the potential metabolite in at least 2 out of the 3 replicates in one of the conditions; (4) ensure a minimum score value (mass accuracy, isotopic pattern) of 70 %. Once the metabolites were identified with good quality parameters, the findings were compared with the available literature and their MS/MS spectra were interpreted to propose the structure. Finally, the potential metabolites were categorized based on the identification confidence level in accordance with the proposal of Schymanski et al. [25].

2.5.2. Non-target screening

A previously developed non-target screening workflow was used to this dataset, using MZmine v2.53 for data processing, R software for statistical analysis and MassHunter Qualitative Analysis software 10.0 for compound identification [19,26].

First, *m/z* features were identified, and the chromatograms were constructed with the module *ADAP Chromatogram Builder*. Next, data were simplified through deconvolution (with *noise amplitude algorithm)* and deisotoping processes and subsequently, chromatographic peaks were aligned across samples using the *RANSAC aligner*. Finally, missing peaks were found using the module *gap filling* and *m/z* features were analyzed in R software using a custom script [27]. Volcano plots were constructed comparing fold changes (FC) obtained between sample groups and negative controls against p-values from a student t-test ($\alpha = 0.05$). Data points with p-value < 0.05 and a log10 FC > 1 were selected for further characterization in MassHunter Qualitative Analysis software, following the identification criteria stablished for suspect screening workflow.

2.6. Quality control

To prevent false positives during the assays, negative controls were incorporated into both Phases (see Figs. S1 and S2). For Phase I, three negative controls were prepared without one of the components of the reaction mixture: substrate (substrate negative control, SNC), HLM (HLM negative control, HNC), and NADPH (cofactor negative control, CNC). Two sets of controls were prepared and incubated for either 1h (SNC-1h, HNC-1h and CNC-1h) or 3h (SNC-3h, HNC-3h and CNC-3h) to monitor reactions of Sets A (1 h) and B (3 h) (Fig. S1). For Phase II, two negative controls for each type of Phase II conjugation were prepared without one of the components of the reaction mixture: substrate (SNC) and cofactor (CNC, UDPGA for GLU and PAPS for SUL) (Fig. S2). The absence of the identified metabolites was confirmed in these negative controls.

In addition, positive control was included to validate the proper course of the Phase I and Phase II reactions (see Figs. S1 and S2). Positive control was prepared using the same reaction media as described in section 2.2 but with a substrate of known metabolism. Phenacetin (100 ng μL^{-1} in TRIS buffer) was used as the Phase I positive control, while 4-NP (1390 ng μL^{-1} in TRIS buffer) was used as the Phase II positive control. Phenacetin undergoes Phase I metabolism resulting in two primary metabolites: N-(4-hydroxyphenyl)-acetamide (P-M1) and N-(4-ethoxyphenyl)-N-hydroxyacetamide (P-M2) [28,29] (Fig. S3). Similarly, 4-NP undergoes Phase II metabolism to form 4-NP glucuronide (4NP-G) and 4-NP sulfate (4NP-S) [30,31] (Fig. S4). All positive control metabolites were detected verifying the good performance of the proposed *in-vitro* assay.

Additionally, instrumental precision was evaluated by examining the variation in area of the IS (Ib-d4), ensuring that the standard deviation of the peak area remained below 10 % in all samples.

2.7. In-silico toxicity assessment

The U.S Environmental Protection Agency Toxicity Estimation Software Tool (TEST) version 5.1 was used to predict (eco)toxicity of DPG, DTG and the tentatively identified metabolites according to quantitative-structure property relationships (QSAR) by the consensus method as it was carried out by Sieira et al. [21]. The toxicological endpoints selected were the oral rat 50 % lethal dose (LD_{50}, as a proxy of human toxicity), 48 h *Daphnia Magna* 50 % lethal concentration (LC_{50}), 48 h *Tetrahymena pyriformis* 50 % growth inhibition concentration (IGC_{50}) and Ames mutagenic test model. On the other hand, the Endocrine Disruptome online platform was used to predict the affinity of target chemicals with human nuclear receptors [32].

3. Results and discussion

3.1. In-vitro metabolic profile

A reduction in DPG and DTG signal was observed in Phase I (Set A and B), Phase II with GLU (set D.1) and Phase I + II (set C.1 and C.2) *in-vitro* metabolism compared to the negative controls, indicating metabolism of both compounds (Fig. 2). However, no significant reduction in signal was observed in only Phase II with SUL experiments (set D.2) (Fig. 2). These observations were confirmed after performing statistical analysis in R, where the Phase I volcano plots (Figs. S5 and S6) showed multiple features meeting the

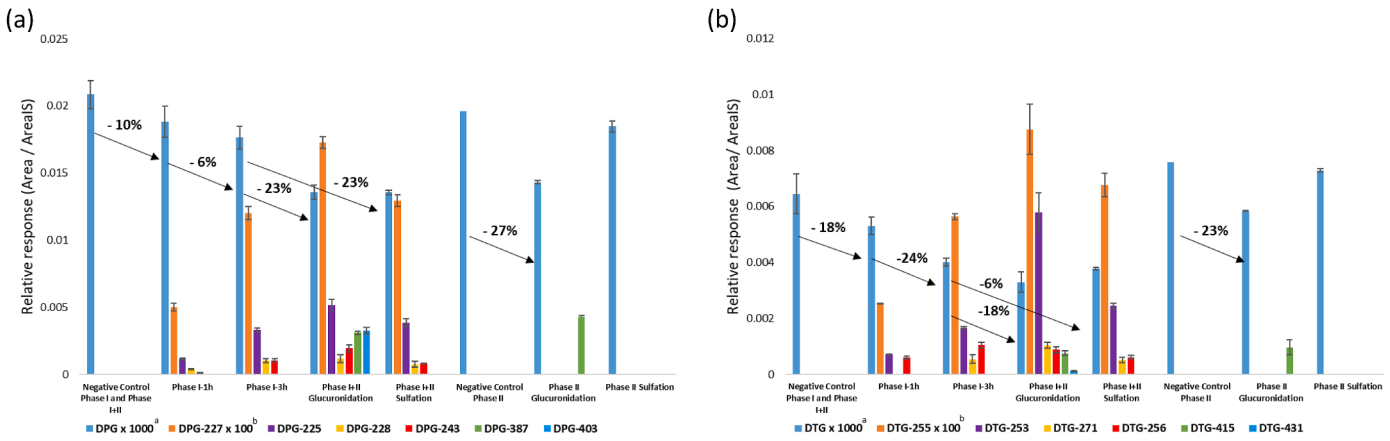

Fig. 2. Trends observed for DPG and their metabolites (a) and DTG and their metabolites (b) in relative response (to IS) during incubation period.

established criteria (p-value <0.05 and a log10 FC > 1), while according to Phase II volcano plots (Figs. S7 and S8) only features from the GLU experiments were statistically significant. Moreover, an increase in the metabolism rate and number of statistically significant features were observed with increasing incubation time of Phase I sets (Fig. 2 and Figs. S5 and S6). During *in-vitro* metabolism Phase II GLU, a reduction in signal was observed in the combined Phase I and II experiments (23 % for DPG and 18 % for DTG) and in the Phase II GLU only experiments (27 % for DPG and 23 % for DTG). On the other hand, samples subjected to SUL denoted a signal reduction in the combined Phase I and II experiments with 23 % for DPG and 6 % for DTG whereas, Phase II SUL only experiments did not show remarkable DPG biotransformation (Fig. 2).

All metabolites were identified through the suspect screening approach outlined in Section 2.5, while the non-target screening workflow was used to verify previous results, as no new metabolites were discovered using this approach. Tables 1 and 2 display the formulae, retention times, ESI mode, mass error, score, double-bond equivalents (DBE) and identification confidence level of the metabolites [25]. Empirical formulae were proposed with a high degree of certainty, with score values above 73 % and mass errors below 5 ppm. The metabolic products were detected consistently in all replicates under the same conditions and were absent in control samples. As some of the MS/MS spectra of these metabolites have not been previously reported in the literature, the proposed structures were based on the interpretation of their MS/MS spectra and from the fragmentation of their precursors (Figs. S9 and S10).

3.1.1. Phase I metabolites

Tables 1 and 2 show that four Phase I *in-vitro* biotransformation products were identified for both DPG and DTG. Phase I metabolism involves three main reactions: hydroxylation, deamination and intramolecular cyclization.

3.1.1.1. Mono and di-hydroxylation. DPG-227 and DTG-255 were detected in both ionization modes as protonated molecular ions (*m/z* 228.1131 and 256.1441, respectively) and in their deprotonated form (*m/z* 226.0975 and *m/z* 254.1298, respectively) and proposed as mono-hydroxylated derivatives, since they contain one additional oxygen atom with respect to the precursor substance (Tables 1 and 2). For DPG-227, two peaks were observed at retention times 5.9 and 6.6 min, which displayed identical fragmentation ions in their MS/MS spectra (Figure S11b). Four peaks were detected for DTG-255 at 6.8, 7.0, 7.4 and 8.4 min. The MS/MS spectrum for the peak at the shortest retention time was different from the other three isomers (Fig. 3). Hydroxylated derivatives have been previously reported as chlorination transformation products by Sieira et al. [21] and in the DPG *in-vitro* study of Clement et al. [15]. The MS/MS spectra (Figures S11b and 3) are mostly in agreement with those reported in the literature [21]. It is suggested that hydroxylation may occur on one of the phenolic rings, most likely in the *para*-position [15]. Nonetheless, the DTG-255 isomer at 6.8 min exhibits a different fragmentation pattern with the most abundant ion fragment resulting from the neutral loss of water and ammonia (Fig. 3). Hence, it is postulated that hydroxylation of the guanidine group may have occurred in that case.

Table 1
Name, chemical formulae, retention time (RT), ESI mode, theoretical *m/z*, mass errors (ppm), score, double bond equivalent (DBE) and identification confidence levels for DPG and their *in-vitro* metabolites.

Name	Chemical formulae	RT[a] (min)	ESI mode	Exact *m/z*	Error[b] (ppm)	Score[c] (%)	DBE	Confidence level
DPG	$C_{13}H_{13}N_3$	7.1	Positive	212.1182	1.5	87	9	1
			Negative	210.1037	1.0	98		
DPG-225	$C_{13}H_{11}N_3O$	6.0	Positive	226.0975	0.88	73	10	3
DPG-227	$C_{13}H_{13}N_3O$	5.9, 6.6	Positive	228.1137	−2.6	96	9	3
			Negative	226.0986	−4.8	87		
DPG-228	$C_{13}H_{12}N_2O_2$	9.9	Negative	227.0826	4.0	88	9	3
DPG-243	$C_{13}H_{13}N_3O_2$	4.5, 5.4	Positive	244.1081	2.5	81	9	3
DPG-387	$C_{19}H_{21}N_3O_6$	5.4	Positive	388.1503	−1.5	82	11	2b
DPG-403	$C_{19}H_{21}N_3O_7$	5.5	Positive	404.1452	−1.5	94	9	3

[a] Only those metabolites for which a good chromatographic peak shape and corresponding MS/MS spectra were found are shown.
[b] As arithmetic mean of the value in detected samples.
[c] A minimum score value of 70 % for mass accuracy and isotopic pattern was used for compound identification.

Table 2
Name, chemical formulae, retention time (RT), ESI mode, theoretical *m/z*, mass errors (in ppm), score, double bond equivalent (DBE) and identification confidence levels for DTG and their *in-vitro* metabolites.

Name	Chemical formulae	RT[a] (min)	ESI mode	Exact *m/z*	Error[b] (ppm)	Score[c] (%)	DBE	Confidence level
DTG	$C_{15}H_{17}N_3$	8.5	Positive	240.1495	2.5	94	9	1
			Negative	238.135	2.0	91		
DTG-253	$C_{15}H_{15}N_3O$	8.9	Positive	254.1288	−3.1	74	10	3
DTG-255	$C_{15}H_{17}N_3O$	6.8, 7.0, 7.4, 8.4	Positive	256.1444	−1.2	90	9	3
			Negative	254.1299	0.17	99		
DTG-256	$C_{15}H_{16}N_2O_2$	11.3	Negative	255.1139	−3.2	92	9	3
DTG-271	$C_{15}H_{17}N_3O_2$	6.0, 7.4	Positive	272.1394	−2.2	79	9	3
DTG-415	$C_{21}H_{25}N_3O_6$	7.1	Positive	416.1816	2.1	82	11	2b
DTG-431	$C_{21}H_{25}N_3O_7$	6.6, 7.8	Positive	432.1765	0.51	84	11	3

[a] Only those metabolites for which a good chromatographic peak shape and corresponding MS/MS spectra were found are shown.
[b] As arithmetic mean of the value in detected samples.
[c] A minimum score value of 70 % for mass accuracy and isotopic pattern was used for compound identification.

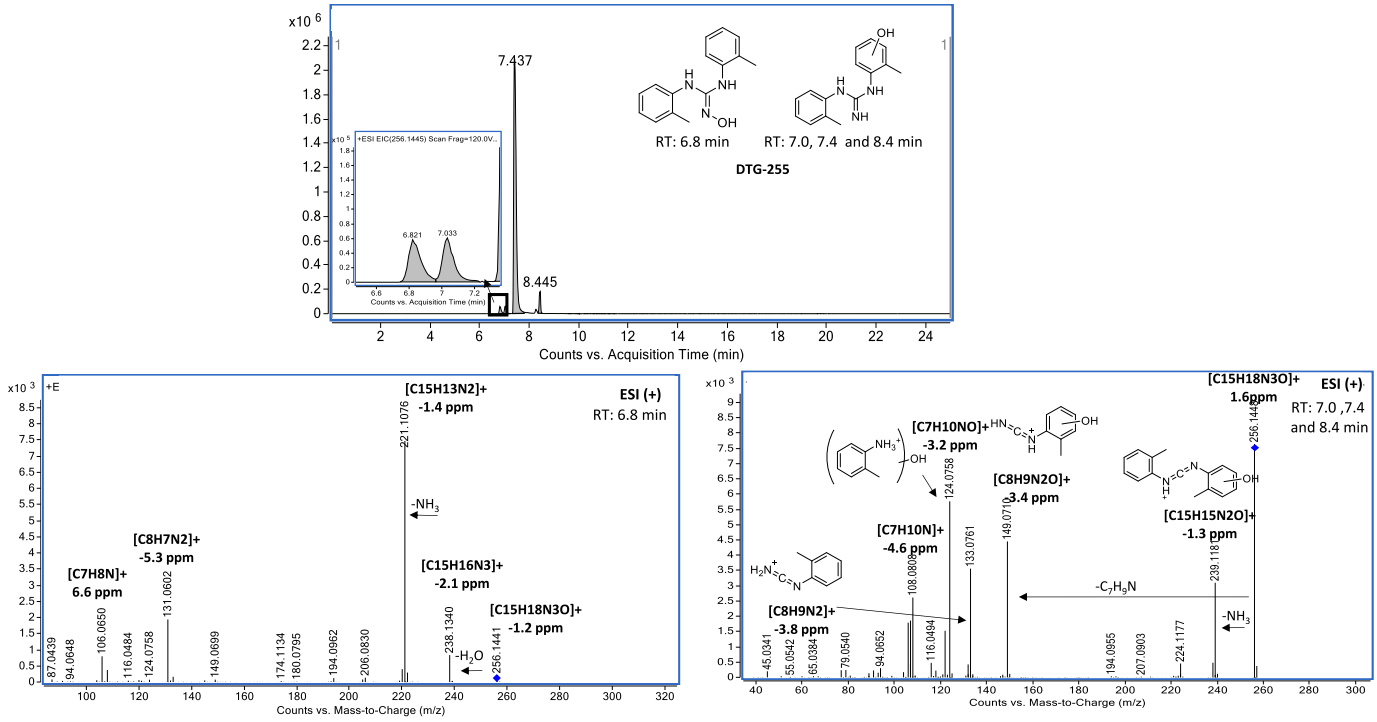

Fig. 3. Extracted ion chromatogram and MS/MS spectra with proposed fragmentation pattern for Phase I DTG-255 metabolite isomers.

DPG-243 and DTG-271 were detected as protonated molecular ions ($[M+H]^+$) (*m/z* 244.1087 and 272.1388, respectively) and proposed as di-hydroxylated metabolites, given that they contain two additional oxygen atoms relative to the original diarylguanidines. Two isomers of DTG-271 with identical MS/MS spectra were identified at 6.0 and 7.4 min (Figure S12c). The MS/MS spectrum (Figure S12c) matches that reported by Sieira et al. as a chlorination transformation product [21]. Analogously, for DPG-243, two chromatographic peaks with very similar MS/MS spectra were also observed with the same *m/z* (4.5 and 5.4 min), pointing again to the existence of two isomers (Figure S11d). The fragmentation pattern was similar to that of the mono-hydroxylated products, sharing common hydroxylated fragment ions, such as *m/z* 135.0556 (N-(hydroxyphenyl) methanediimine) and 110.0597 (aminophenol), but not presenting the non-hydroxylated fragment 119.0604 corresponding to the protonated phenylcarbodiimide (Figure S11d). Therefore, it is postulated that hydroxylation of the two aromatic rings may have occurred.

Consequently, all isomers could be identified as potential Phase I metabolites, although their precise structures could not be elucidated, tentative identification level 3 on the Schymanski scale [21].

3.1.1.2. Deamination followed by oxidation. Both DPG and DTG produced a metabolite with one less N atom and two more O atoms than the precursor substance. The deprotonated molecular ion ($[M-H]^-$) was detected for both products, DPG-228 and DTG-256, with *m/z* values of 227.0817 and 255.1131, respectively (Tables 1 and 2). Only one chromatographic peak was detected for each compound (Figure S11c and S12b). The ESI(−) fragment ions *m/z* 108.0442 for DPG-228 and 122.0603 for DTG-256 and the loss of aniline and toluidine, respectively, also displayed in the mono-hydroxylated metabolites spectra (DPG-227 and DTG-255), were observed, owing to structural similarities. This indicates that the molecules underwent hydroxylation in an aromatic ring. However, the absence of ammonia loss suggests that these molecules contain a urea group rather than the guanidine group (Figures S11b and S12c). Hence, it is suggested that the

guanidine group undergoes deamination, followed by oxidation to form urea, and hydroxylation of an aromatic ring.

3.1.1.3. Intramolecular cyclization. Two products, named DPG-225 and DTG-253, with a similar empirical formula as the hydroxylated metabolites (DPG-227 and DTG-255) but with one additional DBE and 2 less H atoms (Tables 1 and 2), were detected. Several chromatographic peaks were observed with the same *m/z*. However, only the MS/MS spectra for the peak with the highest abundance, at 5.9 min for DPG-225 and at 8.9 min for DTG-253 could be obtained (Figures S11a and S12a). Sieira et al. previously described these products as hydroxylated 7-membered cycle derivatives with a similar fragmentation pattern [21]. However, based on the MS/MS spectra acquired, the position of the hydroxyl group could not be conclusively determined, reaching a tentative identification confidence level of 3 according to Schymaski et al. [25].

3.1.2. Phase II metabolites

The suspect screening approach identified two Phase II *in-vitro* glucuronides for each target compound (Tables 1 and 2). The non-target screening workflow confirmed these metabolites in ESI (+) mode (Figs. S7 and S8). No Phase II *in-vitro* sulfate metabolites were identified, which perfectly matches that no or very few statistical features were found in the Phase II SUL volcano plots (Figs. S7 and S8). The products DPG-387 and DTG-415 were detected, in both only Phase II (Set D.1) and Phase I + II (Set C.1), as protonated molecular ions with *m/z* values of 388.1497 and 416.1817, respectively. These molecular formulae correspond to the addition of $C_6H_8O_6$ (a glucuronide group) (Tables 1 and 2). The most abundant fragment ion, *m/z* 212.1183 for DPG-387 and 240.1505 for DTG-415, correspond to the protonated DPG/DTG molecular ion in both cases, indicating the loss of the glucuronide moiety ($C_6H_8O_6$) (Figures S13a and S14). Moreover, the fragments at *m/z* 270.0966 (DPG-387) and 284.1126 (DTG-415), corresponding to aniline-glucuronide and toluidine-glucuronide respectively, show that the glucuronide group is attached to a N linked to an aromatic ring. This characteristic fragmentation pattern allowed for the tentative identification of the molecules as DPG-N-glucuronide and DTG-N-glucuronide, tentative identification level 2b.

DPG-403 and DTG-431 were identified as protonated forms ($[M+H]^+$, *m/z* 404.1446 and 432.1767, respectively). They have a molecular formula that contains one more O atom than the previous metabolites (DPG-387 and DTG-415) or a glucuronide group ($C_6H_8O_6$) more than the hydroxylated metabolites (DPG-227 and DTG-255). These products were exclusively present in Sample Set C.1, indicating a GLU reaction from the abovementioned Phase I monohydroxylated metabolites (Fig. 2).

DPG-403 exhibited several chromatographic peaks similar to DPG-227 (Figure S13b). However, only the MS/MS spectra for the peak with the highest abundance (at 5.4 min) could be recorded due to the low abundance of the other peaks (Figure S13b). DTG-431 showed two isomers with a differentiated fragmentation pattern at 6.6 and 7.8 min (Fig. 4), in concordance with the different spectra also observed for the hydroxylated derivative (DTG-255). Similar to the N-glucuronide metabolites, DPG-387 and DTG-415, the most intense fragment ions of DPG-403 and DTG-431 isomer at 6.6 min correspond to the protonated molecular ion $[M+H]^+$ of DPG and DTG (Fig. 4 and S13b). However, for the DTG-431 isomer at 7.8 min, the highest observed fragment ion was identified as the protonated mono-hydroxylated DTG (*m/z* 256.1453), indicating the presence of a hydroxy group in the molecule after the cleavage of the glucuronide moiety (Fig. 4). Thus, it is postulated that GLU of the DPG-403 and DTG-431 isomer at 6.6 min occurs on the hydroxy group, while for the DTG-431 isomer at 7.8 min it could occur on the N-group of guanidine. However, the exact position of the glucuronide could not be determined from the MS/MS spectra, so the metabolites were categorized to a tentative identification confidence level of 3.

3.1.3. Biotransformation pathways

In summary, six potential metabolites were identified for each DPG and DTG. All the metabolites were analogous for both compounds, although more hydroxylation isomers were detected in the case of DTG. The response ratio showed that the major oxidative metabolites were the mono-hydroxylated derivatives, DPG-227 and DTG-255 (Fig. 2), as observed in similar studies [17], being the remaining metabolites minor. All Phase I metabolites displayed an increasing signal ratio during the incubation period from 1 h to 3 h (Fig. 2). The biotransformation pathways, as proposed from the structure elucidation, are presented in Fig. 5.

Herein, we propose that the initial step of the *in-vitro* metabolism involves hydroxylation to form DPG-227 and DTG-255. These compounds may undergo three Phase I reactions resulting in the production of the observed minor metabolites: (i) deamination followed by oxidation to obtain DPG-228 and DTG-256, which can also be generated directly from the precursor compound and further hydroxylation; (ii) a second hydroxylation to obtain DPG-243 and DTG-271; and (iii) intramolecular cyclization followed by a hydroxylation to obtain DPG-225 and DTG-253. This cyclization metabolites may have an alternative biotransformation route from the di-hydroxylated metabolites, by elimination of water as proposed by Sieira et al. [21] (Fig. 5).

On the other hand, the formation of the N-glucuronide products (DPG-387 and DTG-415) is postulated to occur directly from the precursor due to the action of UGTs, in accordance with other *in-vitro* metabolism studies [17,33]. This is supported by the detection of the analyte in both sets of samples (C.1 and D.1, Fig. 2). In contrast, the O-glucuronide products (DPG-403 and DTG-431) were only detected in samples subjected to Phase I + II reaction (Set C.1), from the mono-hydroxylated metabolites (Fig. 5).

3.2. In-vivo confirmation and concentration estimates

Urine samples from a non-occupationally adult population were used to confirm *in-vivo* transformation of diarylguanidines into the identified *in-vitro* metabolites. Both deconjugated and non-deconjugated urine set of samples were used to estimate Phase I and Phase II metabolites, respectively. Although the samples were initially screened by LC-QTOF-HRMS, no metabolites could be detected. Therefore, they were again screened by using a target screening methodology by LC-QqQ-MS/MS (see section 2.4 and Text S1), as this system affords much better sensitivity. Moreover. DPG and DTG urinary levels were calculated by the standard addition method.

DPG and DTG were positively detected (in ESI(+)) in all urine pooled samples, with a tolerance of ±30 %, as proposed by Hernández et al. [34] between the Q_1 and any of the qualifiers. Table S4 compiles the concentrations and MS/MS transition ratios (when available) of the diarylguanidines, and their metabolites detected in the urine samples. In general, the concentration levels in the deconjugated set of samples were higher DPG (between 0.040 and 0.119 μg L^{-1}) than DTG (ranging from 0.024 to 0.063 μg L^{-1}) (Table S4). This observation was previously reported in the study of Zhong-Min et al., with DPG urinary levels twice than DTG levels in the United States of America population, although concentration levels reported in that study [35] were considerably higher to those reported in ours. Thus, urinary levels are in line with the higher annual production of DPG [1,2] and

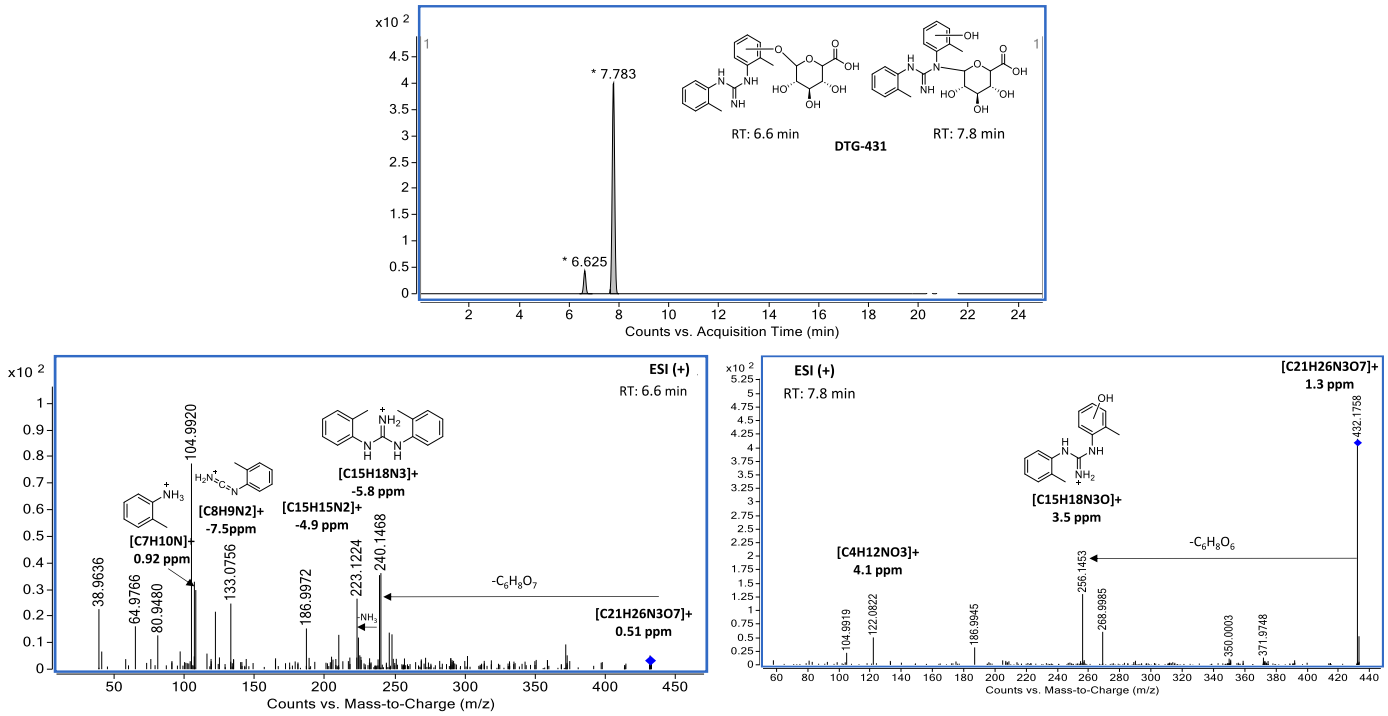

Fig. 4. Extracted ion chromatogram and MS/MS spectra with proposed fragmentation pattern for Phase II DTG-431 metabolite isomers.

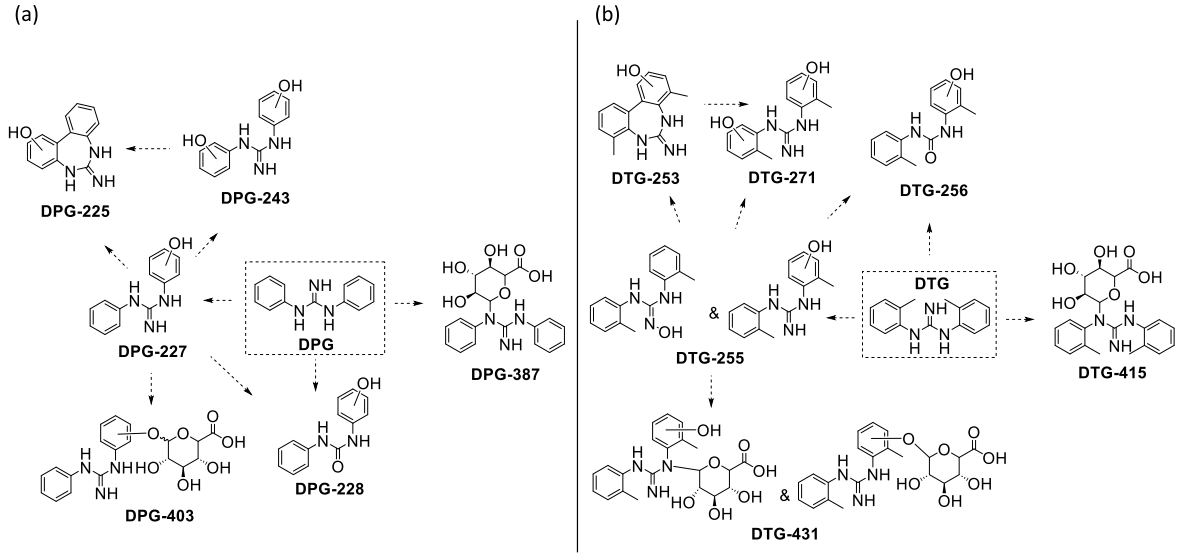

Fig. 5. Proposed *in-vitro* metabolic pathway for DPG (a) and DTG (b).

lower oral bioaccesibility of DTG respective to DPG [36]. On the other hand, an overall upward trend was denoted in the DPG and DTG concentrations for the deconjugated sets of samples (P1d, P2d, P3d and P4d), which potentially indicates the presence of Phase II conjugated metabolites in the urine samples (Table S4).

Three *in-vitro* identified metabolites of DPG were confirmed in the urine samples, whereas none of DTG metabolites could be detected. This fact could be related to the lower levels of exposure to DTG, as stated before, combined with the unknown metabolization and clearance rates. DPG-227 (i.e. mono-hydroxy DPG) was confirmed in all urine samples with the SRM transitions being in the 30 % tolerance margin, in all cases [34]. Fig. 6 shows the comparison between the different transitions obtained for an *in-vitro* metabolism sample and a pooled urine sample. Considering that there was no commercial standards of DPG-227, its urinary concentrations were tentatively estimated using DPG response from the corresponding standard addition curve (Table S4). DPG-227 tentative concentrations were slightly lower than those of DPG, between 0.025 and 0.092 μg L^{-1} in the non-deconjugated set and between 0.049 and 0.101 μgL^{-1} after enzymatic deconjugation, further supporting that it is the major Phase I metabolite of DPG, as reported in the *in-vitro* experiments.

Peaks of the Phase II N-glucuronides DPG-387 and DPG-403 were also detected in the non-deconjugated urine pooled

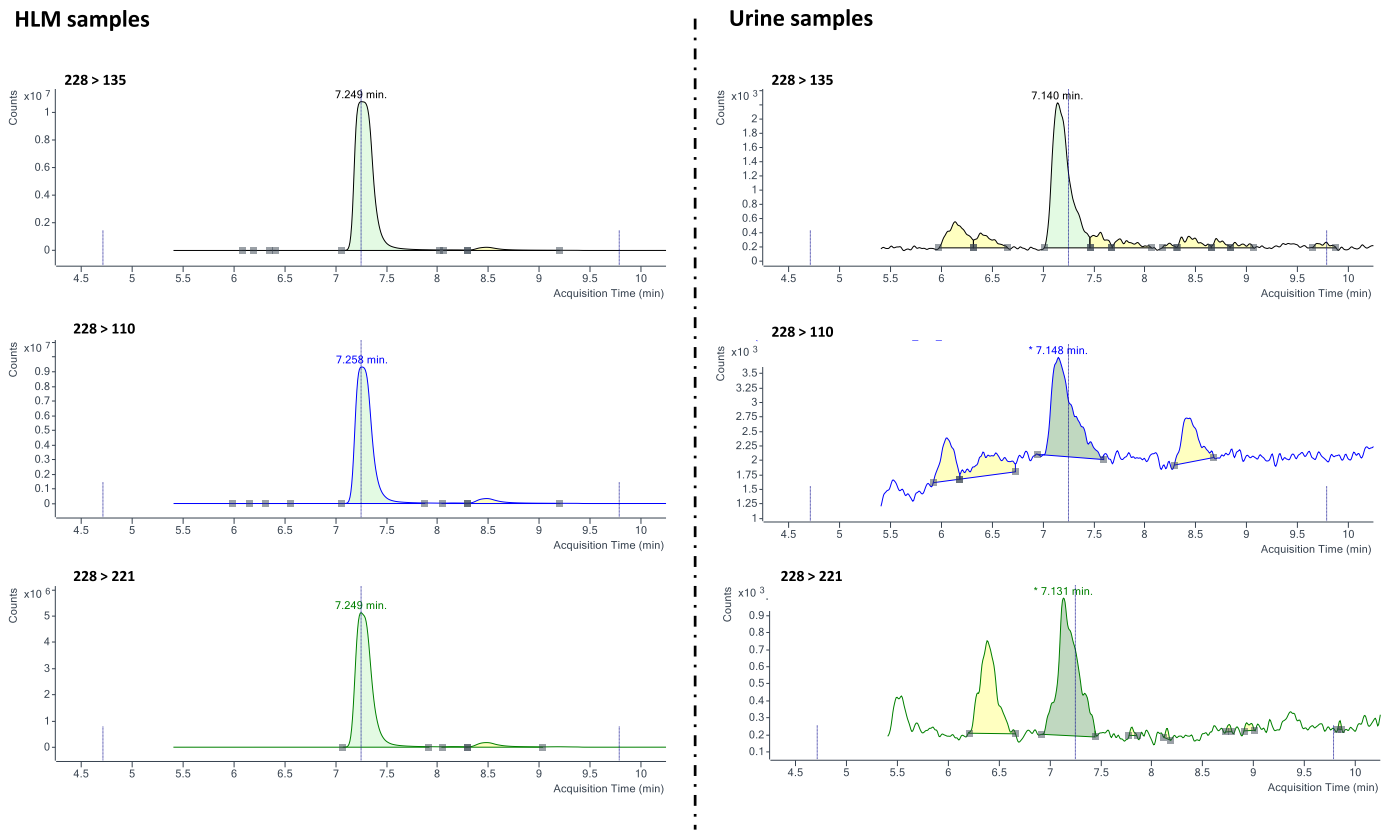

Fig. 6. Chromatographic peaks of MS/MS transitions for DPG-227 found in Phase I in-vitro sets (left) and P1d urine set (right).

samples, although only one MS/MS transition was confirmed (Fig. S15). Nonetheless, as shown in Table S4, the absence of these metabolites in the deconjugated set of samples and the consequent increase of the corresponding deconjugated metabolites (DPG and DPG-227, respectively) further support the identity of these Phase II metabolites, although at very low levels.

Although statistical tests cannot be stablished, DPG levels appear to be slightly higher in the first two set of samples (P1 and P2), corresponding to the male population (Table S4). The study of Zhong-Min et al. also reported significant different levels between adult and children population (with higher levels in infants) and, therefore highlighting the importance of considering factors such as age and gender when carrying out risk assessment for these compounds [20].

3.3. Toxicity assessment

As detailed in Section 2.7, five different *in-silico* (eco)toxicological tests were carried out to predict the toxicity of the diarylguanidines and their metabolic products. Tables 3 and 4 compile the results obtained.

The predicted oral rat LD_{50} toxicities were 499 mg kg^{-1} and 514 mg kg^{-1} for DPG and DTG, respectively, and therefore, both substances are classified in the low-toxicity region (Category 4) according to Ref. [37]. Metabolic products presented even higher LD_{50} values ranging from 1811 to 5477 mg kg^{-1}, denoting low human toxicological hazard (Tables 3 and 4).

As regards acute aquatic toxicities for both endpoints (*Daphnia magna* and *T. pyriformis*), the two diarylguanidines were predicted to have LC_{50} and IGC_{50} values higher than 1 mg L^{-1}. Therefore, they cannot be classified as ecotoxic. Nonetheless, the QSAR predicted toxicity of some DPG and DTG Phase I metabolites for *Daphnia magna* LC_{50}. was slightly lower than that of the original diarylguanidines, but in all cases higher than the ECHA acute ecotoxicity threshold (Tables 3 and 4).

The Ames *in-silico* test revealed a potential mutagenic risk for DPG, DTG, as well as for most metabolites (Tables 3 and 4). A notably high risk was observed for hydroxylated metabolites (with a threshold above 0.8), whereas diarylurea derivatives (DPG-228 and DTG-256) showed no potential mutagenic risk. These results suggest that the guanidine group plays a significant role in the toxicological mechanism. Finally, DTG revealed a high bonding probability with human nuclear receptors (estrogen and mineralcorticoid receptors), a finding also observed in Phase I metabolites of both diarylguanidines showed the high potential to bind with endocrine or androgenic nuclear receptors (Tables 3 and 4), highlighting the importance of including metabolites in the human risk assessment of these chemicals.

4. Concluding remarks

This study presents the first *in-vitro* human liver metabolism assay that tentatively identified structural information of six biotransformation products of each precursor, DPG and DTG, using HRMS. These products include four Phase I metabolites, and two Phase II metabolites formed through processes of hydroxylation, deamination, intramolecular cyclization, and GLU. The monohydroxylated metabolites were found to be the most prominent *in-vitro* metabolites of both DPG and DTG. Furthermore, the hydroxy-phenylurea products (DPG-228 and DTG-256), as well as the glucuronidated conjugates (DPG-387, DPG-403, DTG-415, and DTG-431) were identified for the first time. The *in-vivo* screening

Table 3
Predicted toxicity levels for DPG and its identified metabolites.

Chemical	Oral rat LD_{50} mg kg^{-1}[a]	Daphnia magna LC_{50} (48 h) mg L^{-1}[b]	T. pyriformis IGC_{50} (48 h) mg L^{-1}[c]	Ames mutagenic test Model[e]	Endocrine Disruptome platform[f]
DPG	499	9.12	26.42	0.59	AR (I), PR (I)
DPG-225[d]	Not available	7.62	Not available	0.76	AR (I), ER (I), MR (I), PR (I)
DPG-227[d]	2140	3.95	25.94	0.81	AR (H)
DPG-228[d]	3196	3.59	Not available	0.22	AR (I)
DPG-243[d]	3781	3.96	35.40	0.81	AR (I)
DPG-387	Not available	24.56	Not available	0.75	–
DPG-403[d]	Not available	71.61	Not available	0.73	GR (I)

[a] Amount of chemical (mg kg^{-1} body weight) that causes 50 % of rats to die after oral ingestion.
[b] Concentration of the test chemical in water (mg L^{-1}) that causes 50 % of Daphnia magna to die after 48 h.
[c] Concentration of the test chemical in water (mg L^{-1}) that causes 50 % growth inhibition to Tetrahymena pyriformis after 48 h.
[d] Levels were calculated as a geometrical average of all structural isomers.
[e] US EPA thresholds: <0.5 = non-mutagenic; 0.5–0.8 = potential mutagenic; >0.8 = high mutagenic risk.
[f] High (H), intermediate (I), and low (L) bonding probability of chemical compounds with human nuclear receptors. AR: androgen receptor, PR: progesterone receptor, ER: estrogen receptor, MR: mineralocorticoid receptor, GR: glucocorticoid receptor.

Table 4
Predicted toxicity levels for DTG and its identified metabolites.

Chemical	Oral rat LD_{50} mg kg^{-1}[a]	Daphnia magna LC_{50} (48 h) mg L^{-1}[b]	T. pyriformis IGC_{50} (48 h) mg L^{-1}[c]	Ames mutagenic test model[e]	Endocrine Disruptome platform[f]
DTG	514	3.13	15.47	0.77	AR (I), ER (H), MR (H)
DTG-253[d]	Not available	5.14	7.13	0.82	AR (H), ER (H), MR (H), PR (I)
DTG-255[d]	1811	2.68	16.19	0.80	AR (I)
DTG-256[d]	5477	1.95	Not available	0.22	AR (H), MR (H), ER (H)
DTG-271[d]	1927	2.99	12.22	0.83	AR (I)
DTG-415	Not available	31.03	Not available	0.77	PR (I)
DTG-431[d]	Not available	44.9	Not available	0.67	–

[a] Amount of chemical (mg kg^{-1} body weight) that causes 50 % of rats to die after oral ingestion.
[b] Concentration of the test chemical in water (mg L^{-1}) that causes 50 % of Daphnia magna to die after 48 h.
[c] Concentration of the test chemical in water (mg L^{-1}) that causes 50 % growth inhibition to Tetrahymena pyriformis after 48 h.
[d] Levels were calculated as a geometrical average of all structural isomers.
[e] US EPA thresholds: <0.5 = non-mutagenic; 0.5–0.8 = potential mutagenic; >0.8 = high mutagenic risk.
[f] High (H), intermediate (I), and low (L) bonding probability of chemical compounds with human nuclear receptors. AR: androgen receptor, PR: progesterone receptor, ER: estrogen receptor, MR: mineralocorticoid receptor.

has confirmed the presence of both precursors in human urine samples, with higher urinary levels for DPG. Moreover, three *in-vitro* DPG metabolites (DPG-227, DPG-387 and DPG-403) could be tentatively detected in the biological samples, being DPG-227 confirmed as the major Phase I metabolite of DPG. However, these metabolites and even the original DPG and DTG seem to be present at very low levels. In silico (eco)toxicological predictions point to the need to take metabolites into account in order to estimate the effects of human exposure to these compounds. Yet, further samples from different locations and those related to occupational exposure need to be analyzed to better understand human exposure to these rubber additives. To this end, standards of the major metabolites, and particularly the mono-hydroxylated metabolites need to be produced.

CRediT authorship contribution statement

Andrea Estévez-Danta: Writing – review & editing, Writing – original draft, Validation, Methodology, Investigation, Formal analysis. **Iago Riveiro:** Writing – review & editing, Methodology, Investigation, Formal analysis. **María Lage-Díaz:** Writing – review & editing, Methodology, Investigation, Formal analysis. **José Benito Quintana:** Writing – review & editing, Visualization, Validation, Resources, Funding acquisition, Formal analysis, Conceptualization. **Rosa Montes:** Writing – review & editing, Visualization, Validation, Supervision, Formal analysis, Conceptualization. **Rosario Rodil:** Writing – review & editing, Visualization, Validation, Supervision, Resources, Funding acquisition, Formal analysis, Conceptualization.

Funding information

This research was funded by the Spanish Agencia Estatal de Investigación MCIN/AEI/10.13039/501100011033 (PID2020-117686RB-C32, CNS2024-154426 and TED2021-129200B-C41 (co) funded by the EU through NextGenerationEU/PRTR funds) and Consellería de Cultura de Galicia, Educación e Universidades (ED481A-2020/258, ED431C-2025/21 and ED481B-2025/042).

Declaration of competing interest

The authors declare that they have no known competing financial interests or personal relationships that could have appeared to influence the work reported in this paper.

Acknowledgements

The authors thank “Centro de Supercomputación de Galicia (CESGA)” for the use of their computational resources for HRMS data processing and Agilent for the kind lend of the triple quadrupole LC-MS/MS system.

Appendix. A Supplementary data

Supplementary data to this article can be found online at https://doi.org/10.1016/j.emcon.2025.100551.

References

[1] ECHA, 1,3-di-o-tolylguanidine. https://echa.europa.eu/es/substance-information/-/substanceinfo/100.002.344, 2024. April 2024.
[2] ECHA, 1,3-diphenylguanidine. https://echa.europa.eu/es/substance-information/-/substanceinfo/100.002.730, 2024. April 2024.
[3] R. Montes, R. Rodil, R. Cela, J.B. Quintana, Determination of persistent and mobile organic contaminants (PMOCs) in water by mixed-mode liquid chromatography–tandem mass spectrometry, Anal. Chem. 91 (8) (2019) 5176–5183, https://doi.org/10.1021/acs.analchem.8b05792.
[4] D. Zahn, P. Mucha, V. Zilles, A. Touffet, H. Gallard, T.P. Knepper, T. Frömel, Identification of potentially mobile and persistent transformation products of REACH-registered chemicals and their occurrence in surface waters, Water Res. 150 (2019) 86–96, https://doi.org/10.1016/j.watres.2018.11.042.
[5] H. Tan, L. Yang, Y. Huang, L. Tao, D. Chen, “Novel” synthetic antioxidants in house dust from multiple locations in the asia-pacific region and the United States, Environ. Sci. Technol. 55 (13) (2021) 8675–8682, https://doi.org/10.1021/acs.est.1c00195.
[6] F. Hou, Z. Tian, K.T. Peter, C. Wu, A.D. Gipe, H. Zhao, E.A. Alegria, F. Liu, E. P. Kolodziej, Quantification of organic contaminants in urban stormwater by isotope dilution and liquid chromatography-tandem mass spectrometry, Anal. Bioanal. Chem. 411 (29) (2019) 7791–7806, https://doi.org/10.1007/s00216-019-02177-3.
[7] J. Tang, L. Tang, C. Zhang, G. Zeng, Y. Deng, H. Dong, J. Wang, Y. Wu, Different senescent HDPE pipe-risk: brief field investigation from source water to tap water in China (Changsha City), Environ. Sci. Pollut. Control Ser. 22 (20) (2015) 16210–16214, https://doi.org/10.1007/s11356-015-5275-z.
[8] L. Xie, F. Nakajima, I. Kasuga, F. Kurisu, Simultaneous screening for chemically diverse micropollutants in public water bodies in Japan by high-performance liquid chromatography–Orbitrap mass spectrometry, Chemosphere 273 (2021) 128524, https://doi.org/10.1016/j.chemosphere.2020.128524.
[9] G. Dejonckheere, A. Herman, M. Baeck, Allergic contact dermatitis caused by synthetic rubber gloves in healthcare workers: sensitization to 1,3-diphenylguanidine is common, Contact Dermat. 81 (3) (2019) 167–173, https://doi.org/10.1111/cod.13269.
[10] US-EPA, Substance Evaluation Conclusion as Required by REACH Article 48 and Evaluation Report, 2020 for 1,3-diphenylguanidine (DPG); CAS No: 102-06-7, EC No 203-002-1.
[11] H.M. Shin, C. Moschet, T.M. Young, D.H. Bennett, Measured concentrations of consumer product chemicals in California house dust: implications for sources, exposure, and toxicity potential, Indoor Air 30 (1) (2020) 60–75, https://doi.org/10.1111/ina.12607.
[12] Z.M. Li, K. Kannan, Determination of 1,3-diphenylguanidine, 1,3-Di-o-tolylguanidine, and 1,2,3-triphenylguanidine in human urine using liquid chromatography-tandem mass spectrometry, Environ. Sci. Technol. 57 (24) (2023) 8883–8889, https://doi.org/10.1021/acs.est.3c00412.
[13] P. Che, J.T. Davidson, K. Still, J. Kool, I. Kohler, In vitro metabolism of cathinone positional isomers: does sex matter? Anal. Bioanal. Chem. 415 (22) (2023) 5403–5420, https://doi.org/10.1007/s00216-023-04815-3.
[14] A.L. Phillips, N.J. Herkert, J.C. Ulrich, J.H. Hartman, M.T. Ruis, E.M. Cooper, P. L. Ferguson, H.M. Stapleton, In vitro metabolism of isopropylated and tert-butylated triarylphosphate esters using human liver subcellular fractions, Chem. Res. Toxicol. 33 (6) (2020) 1428–1441, https://doi.org/10.1021/acs.chemrestox.0c00002.
[15] B. Clement, T. Kunze, In vitro oxygenation of N,N'-diphenylguanidines, Xenobiotica 23 (2) (1993) 155–167, https://doi.org/10.3109/00498259309059371.
[16] Y.M. Ioannou, H.B. Matthews, Absorption, distribution, metabolism, and excretion of 1,3-diphenylguanidine in the male F344 rat, Fund. Appl. Toxicol. 4 (1) (1984) 22–29, https://doi.org/10.1016/0272-0590(84)90216-1.
[17] C. Gys, A. Kovačič, C. Huber, F.Y. Lai, E. Heath, A. Covaci, Suspect and untargeted screening of bisphenol S metabolites produced by in vitro human liver metabolism, Toxicol. Lett. 295 (2018) 115–123, https://doi.org/10.1016/j.toxlet.2018.05.034.
[18] N. Van den Eede, W. Maho, C. Erratico, H. Neels, A. Covaci, First insights in the metabolism of phosphate flame retardants and plasticizers using human liver fractions, Toxicol. Lett. 223 (1) (2013) 9–15, https://doi.org/10.1016/j.toxlet.2013.08.012.
[19] P. Vervliet, O. Mortelé, C. Gys, M. Degreef, K. Lanckmans, K. Maudens, A. Covaci, A.L.N. van Nuijs, F.Y. Lai, Suspect and non-target screening workflows to investigate the in vitro and in vivo metabolism of the synthetic cannabinoid 5Cl-THJ-018, Drug Test. Anal. 11 (3) (2019) 479–491, https://doi.org/10.1002/dta.2508.
[20] A. Estévez-Danta, R. Rodil, J.B. Quintana, R. Montes, Determination of the urinary concentrations of six bisphenols in public servants by online solid-phase extraction-liquid chromatography tandem mass spectrometry, Anal. Bioanal. Chem. 416 (20) (2024) 4469–4480, https://doi.org/10.1007/s00216-024-05386-7.
[21] B.J. Sieira, R. Montes, A. Touffet, R. Rodil, R. Cela, H. Gallard, J.B. Quintana, Chlorination and bromination of 1,3-diphenylguanidine and 1,3-di-o-tolylguanidine: kinetics, transformation products and toxicity assessment, J. Hazard Mater. 385 (2020) 121590, https://doi.org/10.1016/j.jhazmat.2019.121590.
[22] Biotranformer, biotranformer 3.0 webpage. https://biotransformer.ca/. April 2024.
[23] QSAR Toolbox, QSAR Toolbox webpage. https://qsartoolbox.org/. April 2024.
[24] C. Stork, G. Embruch, M. Šícho, C. de Bruyn Kops, Y. Chen, D. Svozil, J. Kirchmair, NERDD: a web portal providing access to in silico tools for drug discovery, Bioinformatics 36 (4) (2019) 1291–1292, https://doi.org/10.1093/bioinformatics/btz695.
[25] E.L. Schymanski, J. Jeon, R. Gulde, K. Fenner, M. Ruff, H.P. Singer, J. Hollender, Identifying small molecules via high resolution mass spectrometry: communicating confidence, Environ. Sci. Technol. 48 (4) (2014) 2097–2098, https://doi.org/10.1021/es5002105.
[26] N. Van Wichelen, A. Estévez-Danta, L. Belova, F. den Ouden, N. Verougstraete, M. Roggeman, T. Boogaerts, M. Quireyns, R. Robeyns, N. De Brabanter, J. B. Quintana, R. Rodil, A.L.N. van Nuijs, A. Covaci, C. Gys, In vitro biotransformation of 3-methylmethcathinone (3-MMC) through incubation with human liver microsomes and cytosol and application to in vivo samples, J. Pharmaceut. Biomed. Anal. 248 (2024) 116335, https://doi.org/10.1016/j.jpba.2024.116335.
[27] P. Vervliet, invitRo - in Vitro HLM Assay Feature Prioritization, Zenodo, 2018, https://doi.org/10.5281/zenodo.1253277, v1.0.1.
[28] C. Christia, K.M. da Silva, G. Poma, A.L.N. van Nuijs, A. Covaci, In vitro Phase I metabolism of newly identified plasticizers using human liver microsomes combined with high resolution mass spectrometry and based on non-targeted and suspect screening workflows, Toxicol. Lett. 356 (2022) 33–40, https://doi.org/10.1016/j.toxlet.2021.12.005.
[29] J.A. Hinson, Reactive metabolites of phenacetin and acetaminophen: a review, Environ. Health Perspect. 49 (1983) 71–79, https://doi.org/10.1289/ehp.834971.
[30] N. Gamage, A. Barnett, N. Hempel, R.G. Duggleby, K.F. Windmill, J.L. Martin, M.E. McManus, Human sulfotransferases and their role in chemical metabolism, Toxicol. Sci. 90 (1) (2006) 5–22, https://doi.org/10.1093/toxsci/kfj061.
[31] R.H. Tukey, C.P. Strassburg, Human UDP-glucuronosyltransferases: metabolism, expression, and disease, Annu. Rev. Pharmacol. Toxicol. 40 (2000) 581–616, https://doi.org/10.1146/annurev.pharmtox.40.1.581.
[32] K. Kolšek, J. Mavri, M. Sollner Dolenc, S. Gobec, S. Turk, Endocrine disruptome–an open source prediction tool for assessing endocrine disruption potential through nuclear receptor binding, J. Chem. Inf. Model. 54 (4) (2014) 1254–1267, https://doi.org/10.1021/ci400649p.
[33] H. Frederiksen, N.E. Skakkebaek, A.M. Andersson, Metabolism of phthalates in humans, Mol. Nutr. Food Res. 51 (7) (2007) 899–911, https://doi.org/10.1002/mnfr.200600243.
[34] F. Hernández, D. Fabregat-Safont, M. Campos-Mañas, J.B. Quintana, Efficient validation strategies in environmental analytical chemistry: a focus on organic micropollutants in water samples, Annu. Rev. Anal. Chem. 16 (16) (2023) 401–428, https://doi.org/10.1146/annurev-anchem-091222-112115.
[35] Z.-M. Li, K. Kannan, Determination of 1,3-diphenylguanidine, 1,3-Di-o-tolylguanidine, and 1,2,3-triphenylguanidine in human urine using liquid chromatography-tandem mass spectrometry, Environ. Sci. Technol. 57 (24) (2023) 8883–8889, https://doi.org/10.1021/acs.est.3c00412.
[36] S. Sóñora, A. Duque-Villaverde, D. Armada, T. Dagnac, M. Llompart, In vitro human oral bioaccessibility assessment of hazardous chemicals, including N, N′-substituted-p-phenylenediamines, coming from recycled tire crumb rubber, Chemosphere 367 (2024) 143534, https://doi.org/10.1016/j.chemosphere.2024.143534.
[37] ECHA, Guidance to Regulation (EC) No 1272/2008 on classification, labelling and packaging (CLP) of substances and mixtures, Ref: ECHA-24-G-01-EN. https://doi.org/10.2823/74224, 2024.